DOI: 10.37190/abb/214380

Development of silk vascular graft coated with silk sponge

Takashi Tanaka[1], Tetsuo Asakura[2*]

[1]Department of Veterinary Science, Tokyo University of Agriculture and Technology, Tokyo, Japan

[2]Department of Biotechnology, Tokyo University of Agriculture and Technology, Tokyo, Japan

[*]Corresponding author: Tetsuo Asakura, Department of Biotechnology, Tokyo University of Agriculture and Technology, Tokyo, Japan, e-mail address: asakura@cc.tuat.ac.jp

Submitted: 5th August 2025

Accepted: 17th November 2025

Abstract

Purpose

Changes in diet and lifestyle have increased the number of patients with vascular diseases. Synthetic grafts yield unacceptable outcomes in very small vessels, such as coronary arteries, causing the exclusive use of native vessels despite their limited availability and sometimes suboptimal quality. Therefore, a small-diameter vascular graft that achieves outcomes comparable to native vessels is clinically needed.

Methods

In this paper, porous silk fibroin vascular grafts (PSVG) were prepared using a double-raschel knitting machine to create vascular grafts from silk fibers, followed by coating with a silk sponge using poly(ethylene glycol diglycidyl ether) as a porogen. Gelatin-sealed polyethylene terephthalate vascular grafts and non-porous silk vascular grafts were prepared as controls.

Results

When this PSVG was implanted into rats, positive results were observed at 4 weeks post-implantation. Specifically, endothelial-like cells were confirmed in the central part of the patent PSVG, indicating that endothelialization had progressed within a relatively short period of 4 weeks. However, gelatin-sealed polyethylene terephthalate vascular grafts and non-porous silk vascular grafts showed no indication of the presence of the endothelial-like cells.

Conclusions

These results indicate that PSVG is promising as small-diameter grafts for implantation.

Keywords

porous, silk fibroin, small-diameter vascular graft, polyethylene glycol diglycidyl ether

1. INTRODUCTION

Changes in diet and lifestyle have increased the number of patients with vascular diseases, including arteriosclerosis, which has become a significant issue in modern society [31]. Surgical intervention with bypass grafts may be required in cases of severe vessel occlusion [10]. Synthetic vascular grafts, such as expanded polytetrafluoroethylene (e-PTFE, also known as Gore-Tex®) or woven/knitted polyethylene terephthalate (PET, also known as Dacron®) yarn, are predominantly used for hemodialysis access and larger vessel repairs, but they provide poor patency for small-diameter applications (<6 mm) [17]. Synthetic grafts yield unacceptable outcomes in very small vessels, such as coronary arteries, causing the exclusive use of native vessels despite their limited availability and sometimes suboptimal quality. Therefore, a small-diameter vascular graft that achieves outcomes comparable to native vessels is clinically needed [40].

Different animals, predominantly moth larvae and spiders, produce silk. The best-known moth silk is collected from the pupa of the domesticated silkworm *Bombyx mori*. The silk is composed of two proteins: silk fibroin (SF) and silk sericin (SS) [6]. The silk fibers are inherently tough, making them useful in textile industries after SS removal [18]. Additionally, the SF fibers demonstrate excellent biocompatibility, making them useful as a biomaterial, and have been used in sutures in the surgical field for more than 2,000 years [19]. Furthermore, the SF fibers can be solubilized in concentrate salt solutions, including lithium bromide, lithium thiocyanate, and calcium chloride. Dialysis against water or buffers is utilized to eliminate the salts after solubilization in these solvents. Several different forms from the aqueous solution of SF can be prepared easily, which is one of the excellent SF properties when they are applied as biomaterials

[36]. Additionally, SF that is directly dissolved in organic solvent is prepared in several different forms [13]. SF films are prepared by air-drying the aqueous solutions of SF or the SF dissolved in organic solvent. SF sponges are prepared from the SF solution by freeze-drying or adding salt or sugar particles as porogens. They provide a three-dimensional porous scaffolding material with a large interior surface area and interconnected pore spaces. Non-woven mats and fibers are usually fabricated from SF solutions by electrospinning techniques. Thus, different approaches and methodologies have been utilized to produce silks and silk-based materials with adaptable material forms that target a wide range of applications [1]. These features, together with their tunable mechanical properties, environmental stability, biocompatibility, low immunogenicity, and biodegradability, make SF a promising biomaterial for small-diameter vascular grafts [34].

Our previous studies confirmed that SF grafts are efficient vascular grafts implanted in rat models [8]. A small vessel (1.5 mm in diameter and 10 mm in length) was prepared by repeatedly braiding and winding the fibers. The tubes were then coated with SF gel and implanted into the rat's abdominal aorta. The patency of SF grafts one year after implantation was significantly higher than that of e-PTFE grafts utilized as controls (85.1% vs. 30%, $P < 0.01$) [8]. Endothelial cells and smooth muscle cells (SMCs) migrated into the SF graft early after implantation and organized into endothelial and medial layers, as identified by anti-CD31 or anti-smooth muscle actin immunostaining. The total number of SMCs increased 1.6-fold from 1 month to 3 months. Additionally, vasa vasorum is formed in the adventitia. Sirius-red staining demonstrated the significantly increased collagen content of SF grafts one year after implantation, with a decrease in SF content. Thus, SF may be a promising material for

engineering vascular prostheses for small arteries. SF grafts, in particular, can be utilized as remodeling grafts, which are never observed with polyester or e-PTFE grafts. Several improvements are required from the previous silk grafts to develop small-diameter SF vascular grafts. The strength should be increased while maintaining elasticity, and blood leakage from the graft tube should be prevented, as well as fraying from the ends of the graft.

In this paper, SF grafts of 1.5 mm in diameter and 10 mm in length were prepared by combining double-raschel knitted SF fiber grafts with a coating of SF aqueous solution containing poly(ethylene glycol diglycidyl ether) (PGDE) as a porogen. Min et al [25, 26]. revealed that porous tubular-type SF sponges prepared from the SF aqueous solution with the addition of PGDE as a porogen are flexible and transparent in the hydrated state. These sponges demonstrate excellent mechanical properties, especially high deformation recovery. PGDE is generally utilized as a cross-linking agent for polymer syntheses at temperatures of >60°C, but it was used as a porogen for the SF sponges in their experiments at low temperatures. PGDE is completely removed after immersing the mixed PGDE-SF films in water for three days [9]. Here, the porous SF vascular graft (PSVG) was formed with a double-raschel base and SF/PGDE sponge and assessed *in vivo*. Serious problems were resolved by the coating process in SF vascular graft preparation. Further, we prepared gelatin-sealed PET vascular graft (PETVG) to mimic the large and medium-diameter vascular grafts currently utilized in clinical practice, dried silk on a substrate to develop non-PSVG (NPSVG) and e-PTFE. The implantation findings were then compared with those of PSVG.

2. EXPERIMENTAL

2.1. Preparation and measurement of porous SF sponge pore size

2.1.1 Silk Aqueous Solution Preparation

Silk threads obtained from *B. mori* cocoons were dissolved with calcium chloride ($CaCl_2$; Wako Pure Chemical Industries, Japan) to develop an aqueous solution. The solution was prepared by mixing $CaCl_2$, H_2O, and EtOH in a molar ratio of 1:2:1. Refined silk fibers were added to this solution to create a 10% (w/v) mixture, which was

then stirred and dissolved in a water bath at 70℃ for 1 h. The solution was cooled to room temperature and dialyzed for 3 days with a dialysis membrane, with water changes twice a day (morning and night). The solution was centrifuged at 4℃, 18000 rpm for 30 min after dialysis to remove impurities, causing a silk aqueous solution [39]. The concentration of the solution after dialysis was approximately 5% (w/v), but it could be concentrated by air-drying in the dialysis membrane to obtain a high-concentration silk aqueous solution. Pure water was added to adjust the concentration for lower-concentration solutions. Silk aqueous solutions of approximately 9%, 5%, and 3% (w/v) were prepared and used in the experiments to observe the changes in the pore size of the silk sponge due to different concentrations.

2.1.2 Preparation of porous SF sponge

The SF aqueous solution was mixed with PGDE (Sigma–Aldrich, Japan) in weight ratios of SF:PGDE at 3:1, 2:1, 1:1, 1:2, and 1:3. Each ratio solution was poured into four wells of a 24-well plate and frozen overnight at −20℃. The frozen solid samples were thawed in pure water and retrieved from the wells, then soaked in an excess amount of pure water for 3 days with water changes to remove PGDE [5]. The resulting sponges were then air-dried at room temperature. Sufficient residual PGDE reduction was confirmed with FT-IR.

2.1.3 Measurement of sponge pore size

The air-exposed (upper) and well-contacting (lower) surfaces, as well as the cross-sections of the silk sponges, were observed with a scanning electron microscope (SEM) (VE-7800; KEYENCE, Japan). The diameters of 10 randomly selected pores per sample for porous structures were measured using the measurement software attached to the SEM, and the average diameter was calculated. Data are presented as mean ± standard error. Comparison of means was performed using one-way analysis of variance, followed by the Tukey post-hoc test. Data analysis was performed using the commercial statistics software package GraphPad Prism (Version 5.0a, San Diego, CA, USA). Statistical significance was defined as $P < 0.05$.

2.2. Preparation of PSVG

Raw silk fibers with SS were utilized as the starting materials. Tubes for silk vascular graft with a diameter of 1.5 mm for *in vivo* tests and 4 mm for mechanical property tests were prepared with a computer-controlled double-raschel knitting machine (Fukui Warp

Kitting Co., Ltd., Fukui, Japan) [8]. These double-raschel knitted silk tubes were then degummed in sodium carbonate (0.1% w/v) and Marseille soap (0.2% w/v) solutions at 95°C for 120 min to remove SS from the SF fiber surface. This degumming process was repeated thrice. A 5% SF aqueous solution was mixed with an equal weight of PGDE. A PTFE rod with an inner diameter of 1.5 mm was first inserted into a double raschel silk fibroin (SF) tube. The rod, now encased in the SF tube, was placed inside a cylinder containing a mixed solution of SF and PGDE. The cylinder was then placed in a desiccator and subjected to reduced pressure until all air was removed from the tube. Subsequently, the rod with the SF tube was left to stand overnight at −20°C. Afterward, it was immersed in an excess amount of pure water for three days to remove residual PGDE, with the water being periodically replaced. After natural drying, the rod was removed, and the resulting silk sponge-coated artificial silk graft was sterilized by autoclaving for use in implantation experiments. The removal of PGDE was confirmed using attenuated total reflectance Fourier-transform infrared spectroscopy (AT-FTIR; JASCO) and solid-state NMR measurements under hydrated conditions. Since the outer surface of the coated graft was covered with a thin silk film that blocked the sponge pores, the film was removed using cellophane tape to expose the sponge-like structure. Mechanical properties were evaluated using silk sponge-coated artificial silk grafts prepared by the same method, except with a rod diameter of 4 mm.

2.3. Production of PET vascular graft and non-PSVG

We confirmed the usefulness of silk as a material and the effectiveness of porosity as a structure in developing small-diameter vascular grafts by establishing and comparing them with gelatin-sealed PETVG to mimic the currently clinically applied large and medium-diameter vascular grafts [15] and by drying silk on a substrate to establish NPSVG.

2.3.1 Production of PETVG

A double raschel knit PET tube (Fukui Warp Kitting Co., Ltd., Fukui, Japan), similar to that used for silk artificial vascular scaffolds, was employed as the base material, and low-endotoxin gelatin (NIPPI) was used for coating. Since PET is hydrophobic and may not be compatible with the gelatin solution, the base was pre-soaked in 50% ethanol for 60 min. Gelatin was added to purified water to a final concentration of 1.5% (w/v) and completely dissolved at 60 °C. The PET double raschel, threaded with a 1.5 mm

diameter PTFE rod, was immersed in the gelatin solution. It was then rolled between two plates to allow the gelatin solution to permeate between the fibers. The material was immersed again in the gelatin solution. The sample was then left to stand at 4 °C for several hrs to allow the gelatin to gel. Subsequently, it was immersed in a 10% aqueous glutaraldehyde solution (Wako Pure Chemical Industries) for 60 min. to crosslink the gelatin. To remove the glutaraldehyde, the sample was soaked in 70% ethanol for 30 min, then dried and sterilized by autoclaving.

2.3.2 NPSVG Production

We utilized an aqueous solution prepared by adding approximately 5% (v/v) glycerin (Wako Pure Chemical Industries, Japan) to approximately 7% (w/v) silk aqueous solution for the coating. The silk double-raschel, which was threaded through a PTFE rod with an outer diameter of 1.5 mm, was soaked in the silk solution and rolled between two plates to allow the solution to penetrate the fibers, then dried. This soaking process in the solution and drying was repeated several dozen times to develop a tubular structure of non-porous material. Finally, the structure was sterilized by autoclaving.

2.4. Physical properties

2.4.1 Permeability

The permeabilities of PSVG and PETVG were determined following ISO7198. Both gelatin-sealed and non-sealed PETVG samples were used for PETVG. A water reservoir was connected to a polyethylene tube, followed by the grafts. The water reservoir was designed to apply a hydrostatic pressure of approximately 120 mmHg to the grafts. The water, permeating through the graft walls, was collected and measured in ml/min/cm^2. A comparison of means was performed with a one-way analysis of variance, followed by the Tukey post-hoc test. Mechanical property data analysis was conducted with the commercial statistics software package GraphPad Prism (Version 5.0a, San Diego, CA, USA). *P*-values of <0.05 indicated statistical significance.

2.4.2 Porosity

Porosities of the PSVG and both gelatin-sealed and non-sealed PETVG samples were measured with the liquid displacement method. The scaffold was immersed in a known volume (V_1) of hexane in a graduated cylinder, which was then vacuumed at a 500-hPa vacuum degree for 10 min. V_2 is the total volume of hexane and the hexane-impregnated scaffold. The hexane-impregnated scaffold was then removed from the cylinder, and the

residual hexane volume was recorded as V_3. The total scaffold volume was calculated as ($V = (V_2 - V_1) + (V_1 - V_3) = V_2 - V_3$). Here, ($V_2 - V_1$) represents the tubular scaffold volume and ($V_1 - V_3$) denotes the hexane volume within the scaffold. The porosity of the scaffold (ε) was obtained with the formula (%) = ($V_1 - V_3$)/ ($V_2 - V_1$) × l00.

2.4.3 Suture retention strength

The suture retention strength of PSVG was measured as follows. A nylon 7-0 suture (50–69 μm: k-shirakawa.com, Japan) of PSVG was passed through the graft at a position 2 mm from one end, whereas the other end was fixed to the lower part of a tensile testing machine. The suture was then pulled upward at a 3-mm/min initial speed until the graft tore and the suture detached. The suture retention strength involved the force at this point. The testing machine utilized was an EZ-graph (Shimadzu. co., Japan) with a 100-N load cell.

2.4.4 Compressive strength

An EZ-graph (Shimadzu. co., Japan) with a 5-N load cell was used for determining the compressive strength of PSVG. The measurement was conducted at a compression speed of 2 mm/min. Samples, cut to a 1-cm length, were placed on the testing machine and compressed along the short-axis. The test force is the force applied during compression. The elastic modulus at 25% compression of the diameter (N/mm^2) and the compressive strength at 10% compression of the diameter (N/10%) were calculated with the analysis software TRAPEZIUM (Shimadzu. co., Japan).

2.5. *In vivo* experiments with rats

Female Sprague–Dawley rats weighing 400–500 g were utilized. All rats were housed in cages with a 12-h light/dark cycle. Tokyo University of Agriculture and Technology approved all experimental procedures and protocols (TUAT: Approval number: 23–84), and rats were managed and cared for under the standards established by TUAT and described in its “Guide for the Care and Use of Laboratory Animals.” A PSVG (10 mm long and 1.5 mm inner diameter) was implanted into the rat abdominal aorta, with a diameter of approximately 1.5 mm. Rats were anesthetized by intraperitoneal injection of pentobarbital (50 mg/kg of body weight). The abdominal aorta was exposed, and the aortic branches in this segment were ligated. The proximal and distal portions of the infrarenal aorta were clamped after an intravenous heparin (100 IU/kg) injection. A 10-mm segment of the aorta was removed and replaced by a graft through end-to-end

anastomosis with interrupted 9-0 monofilament nylon sutures (Bear Medic Co, Japan), starting with two stay sutures at 180° to each other, then suturing the front wall, followed by the back wall. Each anastomosis needed 8–10 stitches. The distal, and then proximal vascular clamps, were slowly removed, and flow was restored through the graft. Additionally, NPSVG, PETVG and e-PTFE were implanted for control.

2.6. Histologic and immunohistologic examination

The rats underwent a general physical examination to assess their condition before euthanasia. The rats were perfused with 0.9% saline solution through the left ventricle at the time of death. The grafts, along with the surrounding tissue, were carefully removed, cut transversely at the midline into two pieces, and fixed in methanol for histologic analyses. The methanol-fixed samples were then embedded in paraffin. Paraffin-embedded longitudinal sections (4 μm thick) were processed for hematoxylin and eosin (HE), Masson trichrome (MTC), and endothelial cell (CD31) staining for PSVG. The sections were incubated with primary antibodies against purified mouse anti-rat CD31 (BD biosciences Inc, Japan) followed by incubation with biotinylated anti-mouse immunoglobulin (Ig) G secondary antibody. The avidin–biotin complex technique and diaminobenzidine (DAB) substrate were subsequently utilized. Nuclei were counterstained with hematoxylin. Only HE staining was processed for NPSVG, PETVG and e-PTFE.

2.6.1 HE Staining

HE staining, a commonly used method, was performed to observe the attachment and infiltration of tissue into the grafts to understand the overall tissue structure. The slide glass with the thin-sectioned sample was placed at 60℃ for 1 h to dissolve the paraffin. The paraffin was then completely removed by immersing the sample in xylene for 3 min, thrice. Additionally, it was immersed in methanol for a few seconds, thrice. After washing with running water for 1 min, the sample was placed in Mayer's hematoxylin solution and shaken for 15 min, followed by washing with running water for 10 min. It was then immersed in methanol once, then in eosin solution, and shaken for 6 min. Afterward, it was immersed in methanol for a few seconds, 4 times for differentiation, and then immersed in xylene for a few seconds, thrice for clearing. The sample was then mounted with a mounting medium and cover glass and dried to prepare the sample slide.

2.6.2 MTC Staining

MTC staining is a method that differentiates fibers, including collagen and reticular fibers in blue, nuclei in black-purple, and cytoplasm in light red. The process up to tissue fixation, paraffin embedding, sectioning, and deparaffinization is conducted similarly to other staining methods such as HE staining. The slides with the sections are immersed in a mordant solution and left on a shaker for 30–60 min after deparaffinization and washing of the sections with running water, and then washed with running water for 1 min. The sections are then transferred to Weigert's iron hematoxylin solution and left to stand for 3 min, followed by washing with running water for 1 min and differentiation in 0.1% hydrochloric acid methanol for a few seconds. The sections are immersed in a mordant solution for 45 s after washing with running water for 5 min, and then by another 1 min, and washed with running water. The sections are then immersed in Orange G solution for 5 min, differentiated by immersing in 1% acetic acid water for a few seconds twice, and transferred to Ponceau xylidine acid fuchsin solution, where they are left on a shaker for 3 h. The sections are differentiated by immersing them in 1% acetic acid water for a few seconds twice, then placing them in 2.5% phosphotungstic acid solution and left on a shaker for 2 min. The sections are immersed in aniline blue for 10–20 s after differentiation by immersing in 1% acetic acid water for a few seconds twice, and then by differentiation by immersing in 1% acetic acid water for a few seconds twice. The sections are then dehydrated and cleared by immersing in methanol and xylene for a few seconds, thrice each, and finally mounted with a cover glass and mounting medium.

2.6.3 Endothelial Cell Staining

The process up to deparaffinization is similar to the previously described staining methods. The slide glass was washed with distilled water for 1 min, twice, after deparaffinization and alcohol replacement. Sections were again washed with phosphate-buffered saline (PBS) for 1 min, twice. The slide glass was placed in a moist chamber, and the blocking reagent (10% normal goat serum) was dropped onto the tissue sections, covered with parafilm, and left at room temperature for 10 min. A 50 µL of mouse anti-rat CD31 antibody diluted with PBS was dropped onto each section as the primary antibody, covered with parafilm, and left at 4℃ overnight after removing the blocking reagent. Sections were washed with PBS for 1 min, twice, then the secondary

antibody (biotin-labeled anti-mouse IgG) was dropped, covered with parafilm, and left at room temperature for 10 min. Sections were again washed with PBS, and then peroxidase-labeled streptavidin was dropped, covered with parafilm, and left at room temperature for 10 min. All reagents utilized after the blocking reagent are from a kit (NICHIREI BIOSCIENCES, Japan). After washing with PBS for 1 min, twice, the DAB reagent (NICHIREI BIOSCIENCES, Japan) was dropped and left at room temperature for several minutes while checking the color development under a microscope. Once staining was confirmed, the color development was stopped with distilled water, immersed in hematoxylin solution for a few seconds, and washed with running water for 2 min. Sections were dehydrated, cleared, and mounted.

3. RESULTS

3.1. Porous SF sponge and preparation of PSVG

Figure 1 (a) illustrates the macroscopic view of porous SF sponges formed after mixing with PGDE in weight ratios of SF:PGDE at 3:1, 2:1, 1:1, 1:2, and 1:3, in both wet and dry states. Figure 1 (b) shows the FT-IR spectra of these silk sponges mixed with PGDE before and after washing together with only SF. The IR peaks at 1096.3 and 853.3 cm^{-1}, which characterize the peaks of the epoxy ring, disappeared due to the washing process with water. Thus, PGDE was removed completely after washing, leaving a scaffold material composed of SF. All samples of the mixture of 1% SF and PGDE appear uniform in a wet state but become hard and do not form a sponge-like structure when dried. Furthermore, the samples with 5% SF and PGDE mixed at ratios of 1:3 and 1:2, as well as the samples with 9% SF and PGDE mixed at a ratio of 1:3 also become hard and do not form a sponge-like structure when dried. Figure 2 (a) illustrates the SEM images of the produced sponges, and Table 1 lists the pore sizes measured from these images along with the histograms (Fig. 2 [b]). The pore size measurement results indicated that higher SF concentrations and greater PGDE proportions caused smaller pore sizes. A PSVG could be produced by coating with an SF sponge made according to this method of producing a porous SF sponge (Fig. 3 [a]). However, the outer surface of the PSVG, which was in contact with the tube during preparation, does not form a porous structure as presented in the SEM image of Figure 3 (b). Therefore, the graft was naturally dried after gently washing the graft to prevent significant

structural changes, and then only the surface was peeled off using cellophane tape (Fig. 3 [c]). The SEM images of (Fig. 3 [d]) cross-section and (Fig. 3 [e]) inner surface of the PSVG indeed show that a porous vascular graft has been established.

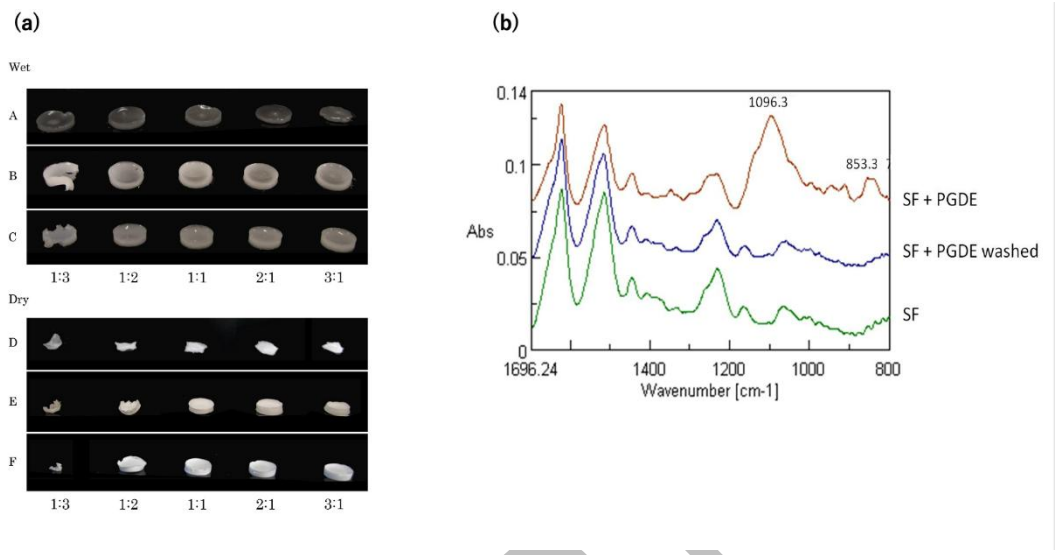

Figure 1. Macroscopic views of silk fibroin (SF) porous sponges prepared with varying silk concentrations - 1 w/v% (A, D), 5 w/v% (B, E) and 9 w/v%. (C, F) - using poly(ethylene glycol diglycidyl ether) (PGDE) as a porogen. The numbers shown below each image indicate the weight ratio of SF to PGDE. Panels A, B, and C show the wet sponges, while panels D, E, and F show the dried sponges. FT-IR spectra of SF/PDFE sponges are presented before washing (SF; PGDE), after washing (SF; PGDE washed), and for pure SF.

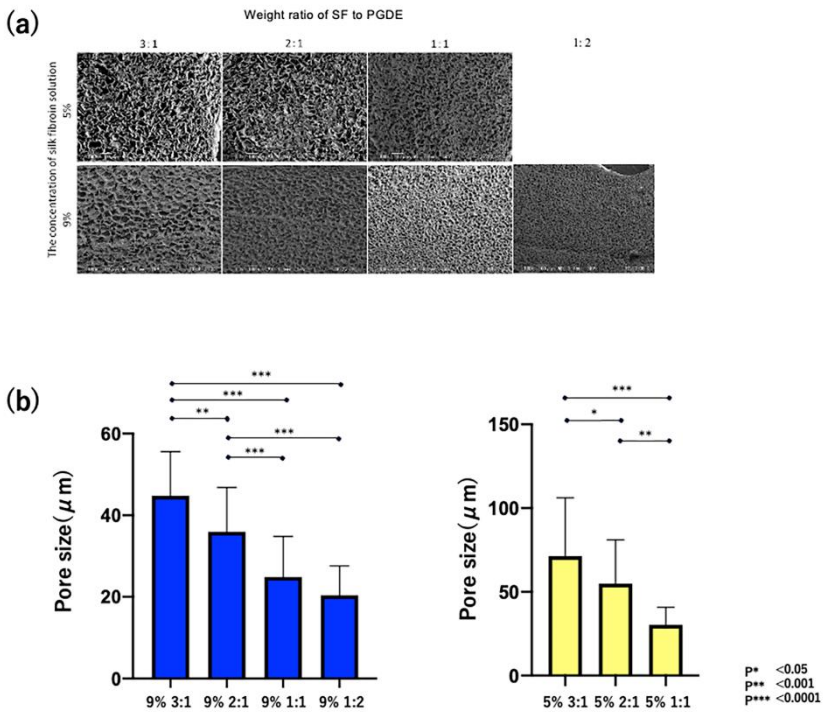

Figure 2. (a) SEM images of poly(ethylene glycol diglycidyl ether) (PGDE)/silk fibroin (SF) sponge cross-sections, showing the weight ratio of SF to PGDE. (b) Histograms of the pore size distribution in SF/PGDE sponges.

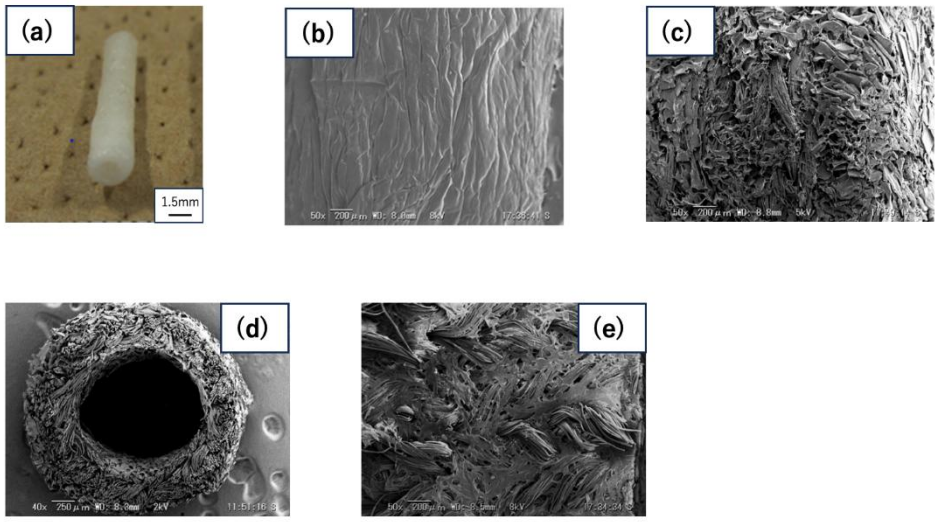

Figure 3. (a) Macroscopic view of porous silk vascular graft (PSVG) and SEM images of (b) the outer surface immediately after fabrication, (c) the outer surface after peeling off the surface with cellophane tape, (d) the graft cross-section, and (e) the graft inner surface.

Table 1. Pore sizes of poly(ethylene glycol diglycidyl ether)(PGDE)/silk fibroin (SF) sponges. Mean±SD

weight ratio of PGDE to SF		1/3	1/2	1	2	3
		Pore size (μm)				
SF(w/v%)	9	44.5±10.9	35.3±10.5	24.9±10.0	20.4±7.2	/
	5	71.4±34.8	54.9±26.1	30.3±10.5	/	/

3.2. Physical properties

Figure 4 (a) illustrates the results of the permeability experiment. PSVG demonstrated an extremely small amount of permeability (62.7 ± 30.3 mL/cm^2/min) compared to the unshielded vascular grafts (387 ± 145 mL/cm^2/min). PSVG permeability was equivalent to that of the gelatin-shielded PETVG (51.7 ± 4.22 mL/cm^2/min). PSVG porosity (82.4 ± 8.41%) was slightly higher than that of gelatin-shielded PETVG (80.6% ± 8.22%) (Fig. 4 [b]). The suture retention strength test was conducted to assess the presence of any issues with operability during surgery or vascular graft separation postoperatively. The results (Fig. 4 [c]) revealed that PSVG had suture retention strength (3.52 ± 0.91N) equivalent to that of native blood vessels (3.0 ± 0.2N). Figure 4 (d) illustrates the progression of the compressive strength during PSVG compression when compressed to 3 mm. The elastic modulus at 25% compression of PSVG was $19.9 \times 10^{-2} \pm 4.56 \times 10^{-3}$ N/mm^2 and compressive strength at 10% compression was $7.70 \times 10^{-2} \pm 5.93 \times 10^{-3}$ N.

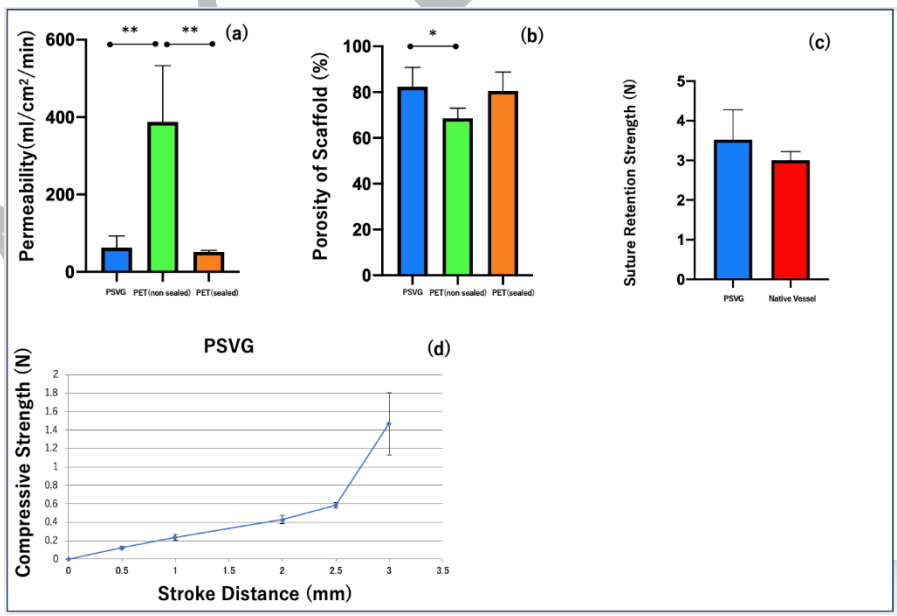

Figure 4. (a) Permeability and (b) porosity of porous silk vascular graft (PSVG) and gelatin-sealed and non-sealed polyethylene terephthalate (PET) grafts, and (c) suture retention strength of PSVG and native

vessels. P* < 0.05, P** < 0.01. (d) The progression of compressive strength (N) of the PSVG when compressed to 3 mm.

3.3. *In vivo* assessment of porous small-diameter silk vascular grafts

The results of the physical property tests indicated that the newly fabricated grafts could withstand *in vivo* experiments, and implantation experiments were conducted on the abdominal aorta of rats (Fig. 5). No difference was observed among the grafts in terms of the ease of handling and resistance to suture. PSVG demonstrated blood soaking into the graft wall and turning it red immediately after clip removal post-implantation due to its sponge-like structure, but no excessive blood leakage was observed, and blood flow was resumed. The patency rates of each graft at four weeks post-implantation were PSVG of 3/4 (75%), NPSVG of 0/4 (0%), PETVG of 0/4 (0%) and e-PTFE of 0/1 (0%). Figure 6 illustrates stained images of NPSVG, PETVG, PSVG and e-PTFE. Spaces in the tissue within the lumen that appeared to be traces of blood flow were observed in the NPSVG, and the lumen of the autologous vessel distal to the heart remained, indicating the presence of a small amount of blood flow. However, a consistent lumen was not present, and it was expected to become completely occluded soon; thus, it was not considered patent. The presence of macrophages and multinucleated giant cells, especially for PETVG (Fig. 6 [e]). Conversely, in PSVG, there are fewer multinucleated giant cells compared to other materials (Fig. 6 [f]). The SF sponge had almost completely lost its structural integrity and was nearly filled with infiltrating cells. Additionally, vascularization was observed in the SF sponge as part of tissue ingrowth. The lumen of the PSVG graft and the anastomosis sites with the native abdominal artery were smooth after four weeks, with no thrombus or intimal hyperplasia observed. Figure 7 (a, b) illustrates images of the MTC stains of longitudinal histological sections of the PSVG. The abdominal implanted SF graft was filled with organized native collagen layers. SF sponge had entirely lost structural integrity and was filled with collagen tissue and penetrated cells. The endothelial cell layer on the PSVG lumen surface was stained with anti-CD31 antibody (Fig. 7 [c]). The endothelial cells fully covered even the center of the PSVG four weeks after implantation in the expanded spectrum (Fig. 7 [d]).

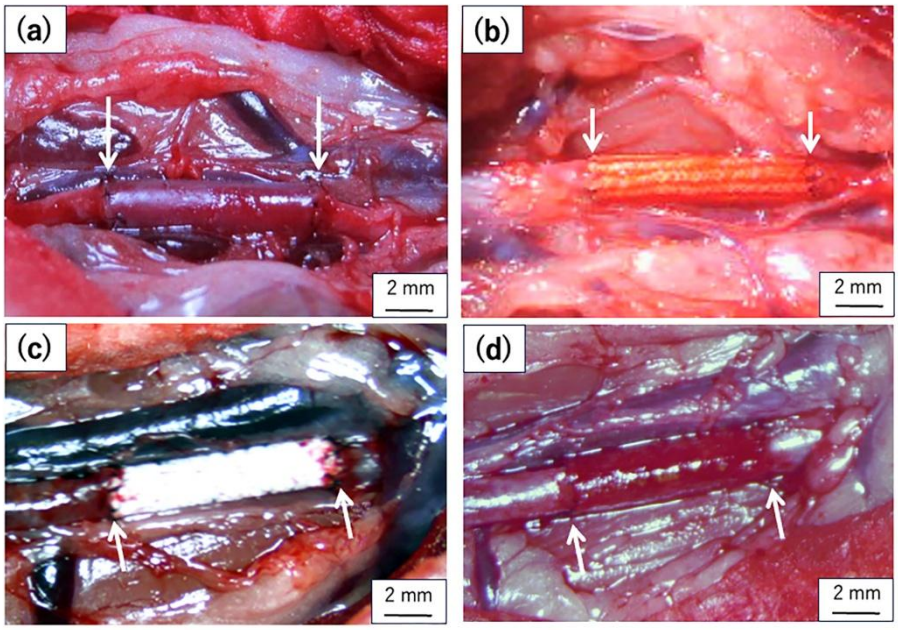

Figure 5. Immediately after graft implantation and reperfusion of three graft types. (a) Non-porous silk fibroin vascular grafts (NPSVG), (b) gelatin-sealed vascular grafts (PETVG), (c) e-PTFE and (d) porous silk vascular grafts (PSVG). White arrows denote the anastomosis sites.

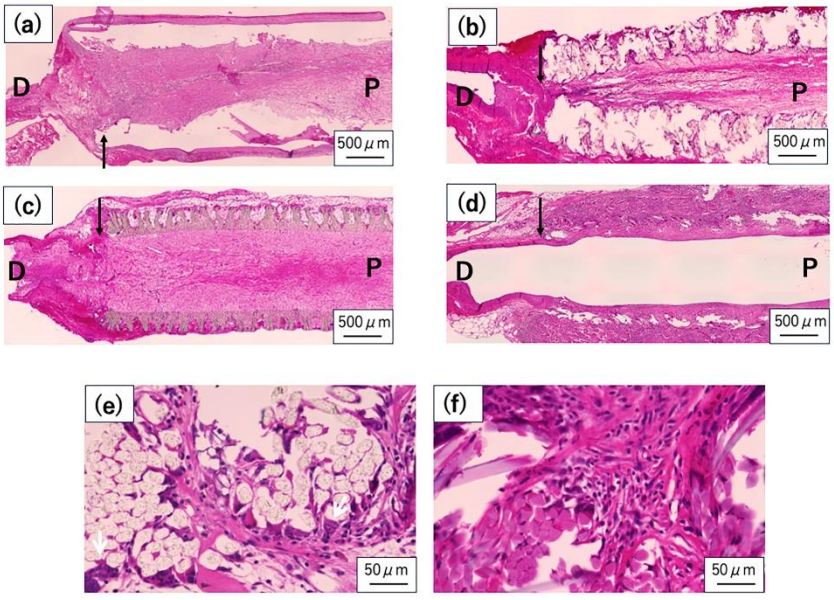

Figure 6. HE stains of longitudinal thin sections of four graft types. (a) Non-porous silk fibroin vascular grafts (NPSVG), (b) gelatin-sealed vascular graft (PETVG), (c) e-PTFE and (d) porous silk vascular graft (PSVG). Black arrows denote the anastomosis sites. Each P and D on the images indicates proximal and distal sides, respectively. Expanded HE stains of (e) gelatin-sealed polyethylene terephthalate vascular graft (PETVG) and (f) porous silk vascular graft (PSVG). The white arrow represents the multinucleated giant cells.

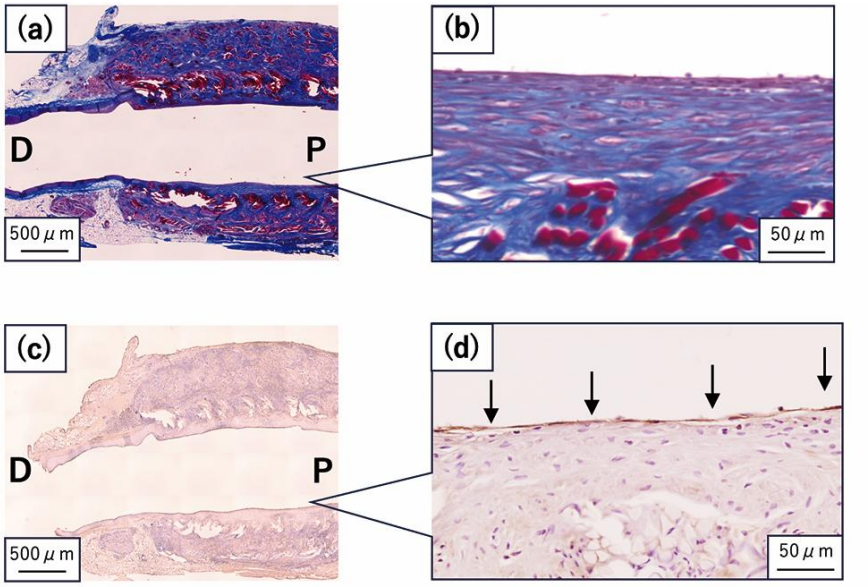

Figure 7. MTC stains of the longitudinal section of (a) porous silk vascular graft (PSVG) and (b) high magnification image of the middle portion. Each P and D on the images indicates proximal and distal sides, respectively. The endothelial cell layer of the lumen surface of PSVG was stained with an anti-CD31 antibody. The image of PSVG (c) longitudinal section, and (d) high magnification image of the middle portion was presented. Arrows represent the lining endothelial cell layer.

4. DISCUSSION

All samples of the mixture of SF and PGDE appear uniform in a wet state but became hard and did not form a sponge-like structure when dried. The overview of these insufficient samples made them unsuitable for producing porous vascular grafts. However, the samples with 5% and 9% SF and PGDE mixed at ratios of above 1:1 appeared uniform in a dry state. The pore size measurement results indicated that higher SF concentrations and greater PGDE proportions caused smaller pore sizes. An additional air-drying process of SF aqueous solution is required to obtain a 9% (w/v) solution. A 5% SF: PGDE of 1:1 solution for sponge production was selected based on these results. The pore size of the coated SF sponge was approximately 30 μm which is expected to be suitable for endothelial cell adhesion and proliferation [27].

PETVG without gelatin shielding requires a pre-clotting process to prevent blood leakage by coagulating blood on the graft wall before transplantation. The results of the permeability experiment indicate a low risk of blood leakage of PSVG during use. Additionally, porosity, which measures the degree of voids in the wall to assess the ease of cell and tissue infiltration into the graft, was also measured. The porosity of scaffold

materials is considered crucial for cell adhesion and tissue infiltration after transplantation, and porosity was measured as an indicator of this degree. Many reports mistakenly equate porosity with permeability in this experiment. However, porosity refers to the void fraction the proportion of void space within the total volume of the scaffold material and is distinct from permeability. The lowest porosity was found in non-shielded PETVG, not because they exhibited fewer voids, but because the unprocessed material demonstrated larger gaps, preventing hexane from being retained within the graft wall. These results indicate that PSVG is filled with a sponge, but its tissue infiltration is comparable to or better than that of commercially available vascular grafts. Vascular graft implantation is generally performed with suturing needles and threads; thus, the surgery itself becomes difficult if the vascular graft is prone to fraying or tearing. Additionally, until the tissue supports the graft through the process of the organization after implantation, a risk that the anastomosis site may tear due to blood pressure exists. Therefore, in this study, we measured the strength of PSVG, established with threads of the same material and thickness as those utilized in actual surgeries, to hold the suturing threads. The PSVG had suture retention strength indicating a minimal risk of separation due to unraveling during surgery or tearing at the suture site due to blood pressure postoperatively. In particular, the risk of SF grafts fraying from the ends because of oblique or longitudinal cutting has been prevented. The flexibility of vascular grafts is considered crucial for operability during implantation surgery and for adapting to the pulsatile environment after implantation. Therefore, we conducted a compression test in the short-axis direction as one of the flexibility indicators of the fabricated vascular grafts. The compressive strength of the PSVG at 10% compression was remarkably smaller than that of e-PTFE (0.668 ± 0.27 N/10%) [12]. In addition, the pressure–diameter curve of the PSVG was a typical J-type pattern. This pattern is comparable to that of the native artery. Thus, the SF sponge will provide softness to the graft.

The result of the patency rates of each graft indicates that, despite creating an artificial vascular graft with SF, which has anti-thrombogenic and biocompatible properties [36], thrombus formation may occur if the artificial vascular graft is not porous. Leakage can be prevented when blood flow is resumed by completely sealing the coated area. However, the hardness of the coated area may have caused thrombus formation caused

by a mismatch in compliance with the native blood vessel [4, 7, 15]. Additionally, the coating that was not easily degraded caused the occlusion, thereby preventing the infiltration of self-tissue after implantation, and hindering the remodeling ability of SF. The graft wall in PETVG was very hard and fell off without being sectioned, causing the graft wall to be absent in the staining results and no stained cells were observed in the detached parts. The gelatin coating decomposed slowly after implantation, thereby preventing sufficient infiltration of inflammatory cells. This caused the collagen fibers to not infiltrate into the gaps in the base of the artificial vascular graft, which may have caused the base to fall off during staining. Gelatin is a collagen derivative and is biocompatible, hydrophilic, and biodegradable [40]. Additionally, gelatin contains a large amount of integrin binding sites, which helps in cell adhesion, migration, and differentiation after implantation [37]. Therefore, the RETVG prepared in this study became occluded after implantation although it is an effective coating material [33]. The polyester base was unable to completely prevent thrombus formation until the inner surface of the artificial vascular graft was covered by vascular endothelial cells after implantation, as the coating material slowly and gradually decomposed after implantation and the base became exposed [11, 20, 32]. Conversely, PSVG demonstrated a relatively high patency rate compared to others. SF fibers, films, powder, or regenerated substrates degrade due to hydrolytic enzymes such as protease and chymotrypsin, which triggers an inflammatory response [14, 21, 24, 38]. Macrophages surround a large, difficult-to-process substance, when present, and fuse to form multinucleated giant cells as shown in the PETVG. Conversely, in PSVG, there were fewer multinucleated giant cells compared to PETVG, and decomposition was more advanced. These results suggest that remodeling into autologous tissue proceeded more quickly in PSVG. In this study, degradation and remodeling of PSVG were evaluated qualitatively based on histological observations. Although Sirius Red staining and quantitative collagen assays were not performed, the observed partial degradation and cellular infiltration after 4 weeks are consistent with the early remodeling phase described by Enomoto et al. [8], in which collagen deposition gradually increased with a decrease in SF content after long-term implantation. The SF in the coating area became porous by mixing SF with PGDE in a 1:1 ratio. This was thought to facilitate inflammatory cell infiltration into the interior of the vascular graft after implantation,

which promotes coating degradation. The infiltration of collagen fibers promotes the endothelialization of vascular grafts [28]; thus, the usefulness of SF + PGDE mixed coating for small-diameter artificial vascular grafts has been demonstrated. A previous study revealed that endothelial cell coverage on the luminal surface of the SF graft was 30%–40% at 2 weeks and nearly 100% at 8 weeks [22]. Neointima formation in implanted artificial vascular grafts may be caused by extension from the anastomosis, capillary origin passing through gaps between the fibers of the graft, and endothelialization due to vascular endothelial progenitor cell adhesion in the circulating blood [29, 23]. In any case, vascular endothelial cells were confirmed in the center of the artificial vascular graft, where it may take the longest time for the endothelium to adhere. The progress after implantation was only observed for up to 4 weeks, but vascular endothelial cells prevent blood vessel lumen narrowing caused by blood clotting and excessive proliferation of SMCs [35]; thus, it was thought that intimal hyperplasia would not occur even if the implantation period was extended. Therefore, PSVG is expected to maintain high patency for a long period after implantation. Several studies have mainly aimed to modify small-diameter vascular grafts through physical, chemical, and biological means to ease early endothelial cell adhesion, migration, and proliferation, and eventually to build an endothelial layer on the surfaces [16]. However, some tissue-engineered vascular graft design strategies have demonstrated greater potential in contrast to autologous or synthetic e-PTFE conduits, but many are still hindered by high production costs which prevent their widespread adoption [30]. The small-diameter artificial vascular graft developed in this study did not require complicated manufacturing processes, such as decellularization, peptide modification, tissue culture, and rapid endothelialization of the graft, which was successfully achieved by applying a porous SF coating. Rapid endothelialization within the lumen site of the graft (generally within 3 months for the grafts that are approximately 1 cm in length) is crucial for implanted graft healing and integration because it stops thrombosis and restenosis [2]. M.A. Al Fahad, et al. designed a novel biocompatible, hemocompatible, and mechanically strong bi-layered small-diameter vascular graft. The harvested grafts demonstrated SMC regeneration and complete endothelialization on the graft lumen after 3 months. However, endothelialization was incomplete in some areas after 1 month

[3]. In conclusion, an affordable, easily reproducible, and biocompatible system is a potential candidate for small-diameter vascular graft reconstruction and repair.

5. CONCLUSIONS

A silk sponge favorable for endothelial cell migration was created after freezing a sample mixed at a 1:1 ratio of 5% silk aqueous solution and PGDE and then removing the PGDE. A PSVG was produced by coating the silk vascular graft made using a double-raschel knitting machine with the same silk sponge under similar conditions. Good results were obtained at 4 weeks post-implantation when this PSVG was implanted into rats. Namely, no significant stenosis was found even at the anastomosis site, and the intima of the same thickness as the autologous vessel continued to the inner wall of the graft. MTC staining results of the PSVG indicated that fibrous tissue infiltrated the graft wall, thereby promoting extracellular matrix-like structure formation. Additionally, the presence of endothelial-like cells was confirmed in the central part of the patent PSVG, indicating that endothelialization had progressed within a relatively short period of 4 weeks. Conversely, PETVG mimicking the gelatin-sealed PETVG currently used clinically for large and medium-diameter sites, e-PTFE and non-PSVGs, all became occluded at 4 weeks post-implantation in rats. These results indicate that PSVG is promising as small-diameter grafts for implantation.

6. Acknowledgement

We acknowledge Prof. Makoto Kodama (Kyushu Institute of Technology) for giving us e-PTFE tube with diameter 1.5 mm.

REFERENCES

[1] AIGNER T.B., DESIMONE E., SCHEIBEL T., *Biomedical applications of recombinant silk-based materials*, Advanced materials 2018, 30 (19), 1704636.

[2] AL FAHAD M.A., LEE H.-Y., PARK S., CHOI M., SHANTO P.C., PARK M. et al.,

Small-diameter vascular graft composing of core-shell structured micro-nanofibers loaded with heparin and VEGF for endothelialization and prevention of neointimal hyperplasia, Biomaterials 2024, 306, 122507.

[3] AL FAHAD M.A., RAHAMAN M.S., MAHBUB M.S.I., PARK M., LEE H.Y., LEE B.T., *Endothelialization and smooth muscle cell regeneration capabilities of a bi-layered small diameter vascular graft for blood vessel reconstruction*, Mater Design 2023, 225.

[4] AO P., HAWTHORNE W., VICARETTI M., FLETCHER J., *Development of intimal hyperplasia in six different vascular prostheses*, European Journal of Vascular and Endovascular Surgery 2000, 20 (3), 241–249.

[5] ASAKURA T., ENDO M., FUKUHARA R., TASEI Y., *13 C NMR characterization of hydrated 13 C labeled Bombyx mori silk fibroin sponges prepared using glycerin, poly (ethylene glycol diglycidyl ether) and poly (ethylene glycol) as porogens*, Journal of Materials Chemistry B 2017, 5 (11), 2152–2160.

[6] ASAKURA T., KAPLAN D.L., *Encyclopedia of Agricultural Science*, Academic Press, London 1994.

[7] BOS G.W., POOT A.A., BEUGELING T., VAN AKEN W., FEIJEN J., *Small-diameter vascular graft prostheses: current status*, Archives of Physiology and Biochemistry 1998, 106 (2), 100–115.

[8] ENOMOTO S., SUMI M., KAJIMOTO K., NAKAZAWA Y., TAKAHASHI R., TAKABAYASHI C. et al., *Long-term patency of small-diameter vascular graft made from fibroin, a silk-based biodegradable material*, Journal of vascular surgery 2010, 51 (1), 155–164.

[9] FUKAYAMA T., TAKAGI K., TANAKA R., HATAKEYAMA Y., AYTEMIZ D., SUZUKI Y.

et al., *Biological reaction to small-diameter vascular grafts made of silk fibroin implanted in the abdominal aortae of rats*, Annals of vascular surgery 2015, 29 (2), 341–352.

[10] HARSKAMP R.E., LOPES R.D., BAISDEN C.E., DE WINTER R.J., ALEXANDER J.H., *Saphenous vein graft failure after coronary artery bypass surgery: pathophysiology, management, and future directions*, Annals of surgery 2013, 257 (5), 824–833.

[11] HARUGUCHI H., TERAOKA S., *Intimal hyperplasia and hemodynamic factors in arterial bypass and arteriovenous grafts: a review*, Journal of Artificial Organs 2003, 6 (4), 227–235.

[12] HAYASHI F., OKUDA Y., NAKATA M., NATORI K., *Development of a Small-Diameter Expanded Polytetrafluoroethylene Vascular Graft*, SEI TECHNICAL REVIEW-ENGLISH EDITION- 2003, 83–88.

[13] HOLLAND C., NUMATA K., RNJAK-KOVACINA J., SEIB F.P., *The biomedical use of silk: past, present, future*, Advanced healthcare materials 2019, 8 (1), 1800465.

[14] HORAN R.L., ANTLE K., COLLETTE A.L., WANG Y., HUANG J., MOREAU J.E. et al., *In vitro degradation of silk fibroin*, Biomaterials 2005, 26 (17), 3385–3393.

[15] ISENBERG B.C., WILLIAMS C., TRANQUILLO R.T., *Small-diameter artificial arteries engineered in vitro*, Circulation research 2006, 98 (1), 25–35.

[16] JANA S., *Endothelialization of cardiovascular devices*, Acta biomaterialia 2019, 99, 53–71.

[17] KAWECKI F., L'HEUREUX N., *Current biofabrication methods for vascular tissue engineering and an introduction to biological textiles*, Biofabrication 2023, 15 (2), 022004.

[18] KOH L.-D., CHENG Y., TENG C.-P., KHIN Y.-W., LOH X.-J., TEE S.-Y. et al., *Structures, mechanical properties and applications of silk fibroin materials*, Progress in Polymer Science 2015, 46, 86–110.

[19] KUNDU B., KURLAND N.E., BANO S., PATRA C., ENGEL F.B., YADAVALLI V.K. et al., *Silk proteins for biomedical applications: Bioengineering perspectives*, Progress in polymer science 2014, 39 (2), 251–267.

[20] KUWABARA F., NARITA Y., YAMAWAKI-OGATA A., SATAKE M., KANEKO H., OSHIMA H. et al., *Long-term results of tissue-engineered small-caliber vascular grafts in a rat carotid arterial replacement model*, Journal of Artificial Organs 2012, 15 (4), 399–405.

[21] LI M., OGISO M., MINOURA N., *Enzymatic degradation behavior of porous silk fibroin sheets*, Biomaterials 2003, 24 (2), 357–365.

[22] LOVETT M., ENG G., KLUGE J., CANNIZZARO C., VUNJAK-NOVAKOVIC G., KAPLAN D.L., *Tubular silk scaffolds for small diameter vascular grafts*, Organogenesis 2010, 6 (4), 217–224.

[23] MAHARA A., SOMEKAWA S., KOBAYASHI N., HIRANO Y., KIMURA Y., FUJISATO T. et al., *Tissue-engineered acellular small diameter long-bypass grafts with neointima-inducing activity*, Biomaterials 2015, 58, 54–62.

[24] MEINEL L., HOFMANN S., KARAGEORGIOU V., KIRKER-HEAD C., MCCOOL J., GRONOWICZ G. et al., *The inflammatory responses to silk films in vitro and in vivo*, Biomaterials 2005, 26 (2), 147–155.

[25] MIN S., GAO X., HAN C., CHEN Y., YANG M., ZHU L. et al., *Preparation of a silk fibroin spongy wound dressing and its therapeutic efficiency in skin defects*, Journal of Biomaterials Science, Polymer Edition 2012, 23 (1-4), 97–110.

[26] MIN S., GAO X., LIU L., TIAN L., ZHU L., ZHANG H. et al., *Fabrication and characterization of porous tubular silk fibroin scaffolds*, Journal of Biomaterials Science, Polymer Edition 2009, 20 (13), 1961–1974.

[27] NARAYAN D., VENKATRAMAN S., *Effect of pore size and interpore distance on endothelial cell growth on polymers*, Journal of Biomedical Materials Research Part A: An Official Journal of The Society for Biomaterials, The Japanese Society for Biomaterials, and The Australian Society for Biomaterials and the Korean Society for Biomaterials 2008, 87 (3), 710–718.

[28] NOISHIKI Y., TOMIZAWA Y., YAMANE Y., MATSUMOTO A., *Autocrine angiogenic vascular prosthesis with bone marrow transplantation*, Nature medicine 1996, 2 (1), 90–93.

[29] NOISHIKI Y., YAMANE Y., TOMIZAWA Y., MATSUMOTO A., *Transplantation of autologous tissue fragments into an e-PTFE graft with long fibrils*, Artificial Organs 1995, 19 (1), 17–26.

[30] OBIWELUOZOR F.O., EMECHEBE G.A., KIM D.-W., CHO H.-J., PARK C.H., KIM C.S. et al., *Considerations in the development of small-diameter vascular graft as an alternative for bypass and reconstructive surgeries: a review*, Cardiovascular Engineering and Technology 2020, 11 (5), 495–521.

[31] PASHNEH-TALA S., MACNEIL S., CLAEYSSENS F., *The tissue-engineered vascular graft—past, present, and future*, Tissue Engineering Part B: Reviews 2016, 22 (1), 68–100.

[32] PEKTOK E., NOTTELET B., TILLE J.-C., GURNY R., KALANGOS A., MOELLER M. et al., *Degradation and healing characteristics of small-diameter poly (ε-caprolactone) vascular grafts in the rat systemic arterial circulation*, Circulation

2008, 118 (24), 2563–2570.

[33] POK S., MYERS J.D., MADIHALLY S.V., JACOT J.G., *A multilayered scaffold of a chitosan and gelatin hydrogel supported by a PCL core for cardiac tissue engineering*, Acta biomaterialia 2013, 9 (3), 5630–5642

[34] SETTEMBRINI A., BUONGIOVANNI G., SETTEMBRINI P., ALESSANDRINO A., FREDDI G., VETTOR G. et al., *In-vivo evaluation of silk fibroin small-diameter vascular grafts: State of art of preclinical studies and animal models*, Frontiers in Surgery 2023, 10, 1090565.

[35] TAI N., SALACINSKI H., EDWARDS A., HAMILTON G., SEIFALIAN A., *Compliance properties of conduits used in vascular reconstruction*, Journal of British Surgery 2000, 87 (11), 1516–1524.

[36] VEPARI C., KAPLAN D.L., *Silk as a biomaterial*, Progress in polymer science 2007, 32 (8-9), 991–1007.

[37] XIANG P., WANG S.-S., HE M., HAN Y.-H., ZHOU Z.-H., CHEN D.-L. et al., *The in vitro and in vivo biocompatibility evaluation of electrospun recombinant spider silk protein/PCL/gelatin for small caliber vascular tissue engineering scaffolds*, Colloids and Surfaces B: Biointerfaces 2018, 163, 19–28.

[38] XU W., KE G., PENG X., *Studies on the effects of the enzymatic treatment on silk fine powder*, Journal of applied polymer science 2006, 101 (5), 2967–2971.

[39] YOSHIMIZU H., ASAKURA T., *Preparation and characterization of silk fibroin powder and its application to enzyme immobilization*, Journal of applied polymer science 1990, 40 (1-2), 127–134.

[40] ZHU C., FAN D., WANG Y., *Human-like collagen/hyaluronic acid 3D scaffolds for vascular tissue engineering*, Materials Science and Engineering: C 2014, 34,

393–401.